Mitochondria-mediated apoptosis by diallyl trisulfide in human prostate cancer cells is associated with generation of reactive oxygen species and regulated by Bax/Bak

Young-Ae Kim, Dong Xiao, Hui Xiao, Anna A. Powolny, Karen L. Lew, Megan L. Reilly, Yan Zeng, Zhou Wang, and Shivendra V. Singh

Department of Pharmacology and Urology and University of Pittsburgh Cancer Institute, University of Pittsburgh School of Medicine, Pittsburgh, Pennsylvania

Abstract

Garlic constituent diallyl trisulfide (DATS) inhibits growth of cancer cells *in vitro* and *in vivo* by causing apoptosis, but the sequence of events leading to cell death is not fully understood. We now show that DATS treatment triggers mitochondria-mediated apoptosis program in human prostate cancer cells (LNCaP, LNCaP-C81, LNCaP-C4-2) irrespective of their androgen responsiveness. Interestingly, a normal prostate epithelial cell line (PrEC) is significantly more resistant to apoptosis induction by DATS compared with prostate cancer cells. The DATS-induced apoptosis in LNCaP cells correlated with the collapse of mitochondrial membrane potential, modest increase in protein level of Bak, and down-regulation of Bcl-2 and Bcl-xL protein levels. The DATS-induced apoptosis was significantly attenuated by knockdown of Bax and Bak proteins, but not by ectopic expression of either Bcl-2 or Bcl-xL. The DATS treatment caused generation of reactive oxygen species (ROS) in LNCaP cells, but not in PrEC, which was attenuated by pretreatment with antioxidant *N*-acetylcysteine. The *N*-acetylcysteine pretreatment conferred significant protection against DATS-mediated disruption of the mitochondrial membrane potential and apoptosis. In conclusion, the present study reveals that the mitochondria-mediated cell death by DATS is associated with ROS generation and regulated by Bax/Bak but independent of Bcl-2 or Bcl-xL. [Mol Cancer Ther 2007;6(5):1599–609]

Received 12/6/06; revised 2/24/07; accepted 3/27/07.

Grant support: U.S. Public Health Service grant CA113363 awarded by the National Cancer Institute.

The costs of publication of this article were defrayed in part by the payment of page charges. This article must therefore be hereby marked *advertisement* in accordance with 18 U.S.C. Section 1734 solely to indicate this fact.

Requests for reprints: S.V. Singh, 2.32A Hillman Cancer Center Research Pavilion, University of Pittsburgh Cancer Institute, 5117 Centre Avenue, Pittsburgh, PA 15213. Phone: 412-623-3263; Fax: 412-623-7828. E-mail: singhs@upmc.edu

doi:10.1158/1535-7163.MCT-06-0754

Introduction

Epidemiologic data continue to support the premise that dietary intake of *Allium* vegetables such as garlic may reduce the risk of different types of malignancies including cancer of the prostate (1–3). The anticarcinogenic effect of *Allium* vegetables is attributable to organosulfur compounds (4). *Allium* vegetable-derived organosulfur compounds (OSC), including diallyl sulfide, diallyl disulfide, and/or diallyl trisulfide (DATS), have been shown to inhibit cancer in animal models induced by a variety of carcinogens, including tobacco-derived chemicals (5–8). The mechanisms by which OSCs inhibit chemically induced cancer are well studied and involve an increase in expression of phase 2 carcinogen-detoxifying enzymes and inhibition of cytochrome P450–dependent monooxygenases (8–10). We have also shown previously that oral administration of diallyl disulfide significantly inhibits growth of H-*ras* oncogene–transformed tumor xenografts in athymic mice (11).

More recent studies including those from our laboratory have revealed that naturally occurring OSC analogues can inhibit growth of cancer cells by causing G_2 and M phase cell cycle arrest and apoptosis induction (12–20). For example, the diallyl disulfide–induced cell death in colon cancer cells correlated with an increase in the levels of intracellular calcium (12), whereas G_2-M phase cell cycle arrest was accompanied by an increase in cyclin B1 protein level, reduction in complex formation between cyclin-dependent kinase 1 (Cdk1) and cyclin B1, and hyperphosphorylation of Cdk1 (13). We have shown recently that DATS is much more potent than either diallyl sulfide or diallyl disulfide in inhibiting proliferation of human prostate cancer cells (15). We also found that the DATS-treated prostate cancer cells are arrested in both G_2 phase and mitosis (16, 18). The DATS-induced G_2 phase cell cycle arrest in human prostate cancer cells is caused by reactive oxygen species (ROS)–mediated degradation and Ser^{216} phosphorylation of Cdc25C, leading to the inhibition of kinase activity of Cdk1/cyclin B1 complex (16), whereas the mitotic block is linked to the activation of DNA damage checkpoint effector checkpoint kinase 1 (18). The ROS generation by DATS correlates with the degradation of iron storage protein ferritin, leading to an increase in labile (chelatable) iron (20). Despite these advances, however, the mechanism of DATS-induced apoptosis is not fully defined. An understanding of the mechanism by which DATS causes apoptosis is critical for its further development as a clinically useful anticancer agent because this knowledge could lead to the identification of mechanism-based biomarkers potentially useful in future clinical trials.

We have shown previously that DATS causes apoptotic cell death in PC-3 and DU145 human prostate cancer cell lines, which are androgen independent and lack functional p53 (15). However, it is unclear if the apoptosis induction by DATS is restricted to androgen-independent prostate cancer cells. Further studies are also needed to identify the signal(s) that mediate apoptosis program in DATS-treated cells. Here, we provide experimental evidence to indicate that DATS targets mitochondria to trigger cell death in human prostate cancer cells, which correlates with ROS generation and dependent on Bax and Bak proteins.

Materials and Methods

Reagents

DATS (purity ~97%) was purchased from LKT Laboratories. Cell culture reagents and fetal bovine serum (FBS) were from Life Technologies. RNase A was from Promega, 6-carboxy-2′,7′-dichlorodihydrofluorescein diacetate (H_2DCFDA) was from Molecular Probes, and propidium iodide, 4′,6-diamidino-2-phenylindole (DAPI), and *N*-acetylcysteine were from Sigma. The antibodies against Bax, Bak, Bid, Smac/DIABLO, and Bcl-xL were from Santa Cruz Biotechnology; the antibody against actin was from Sigma; the antibody against Bcl-2 was from DakoCytomation; the antibodies against procaspase-3, cytochrome *c*, and cytochrome *c* oxidase IV (COX IV) were from Cell Signaling Technology, BD PharMingen, and Invitrogen, respectively.

Cell Lines and Cell Culture

The LNCaP (American Type Culture Collection), LNCaP-C4-2 (UroCor), and LNCaP-C81 (a generous gift from Dr. Ming-Fong Lin, University of Nebraska, Omaha, NE) were maintained in RPMI 1640 supplemented with 1 mmol/L sodium pyruvate, 10 mmol/L HEPES, 0.2% glucose, 10% (v/v) FBS, and antibiotics. Normal prostate epithelial cell line PrEC was purchased from Clonetics and maintained in PrEBM (Cambrex). The mouse embryonic fibroblasts (MEF) derived from wild-type (WT) and Bak and Bax double knock-out (DKO) mice were maintained as described by Wei et al. (21). Stock solution of DATS was prepared in DMSO, and an equal volume of DMSO (final concentration 0.2%) was added to the controls.

Measurement of Apoptosis and Cell Viability

The DATS-induced apoptosis was determined by (*a*) fluorescence microscopy after staining the cells with DAPI, (*b*) analysis of cytoplasmic histone-associated DNA fragmentation, or (*c*) analysis of subdiploid fraction by flow cytometry after staining the cells with propidium iodide essentially as described previously (15, 16, 18, 19). Cell viability was determined by trypan blue dye exclusion assay as described previously (15).

Transmission Electron Microscopy and Mitochondria Membrane Potential Assay

Transmission electron microscopy in LNCaP cells treated with DMSO (control) or 40 μmol/L DATS for 3, 6, 9, or 16 h at 37°C was done as described previously (22). The effect of DATS treatment on mitochondrial membrane potential was measured using a potential-sensitive dye 5,5′,6,6′-tetrachloro-1,1′,3,3′-tetraethyl-benzimidazolylcarbocyanine iodide (JC-1). Stock solution of JC-1 (1 mg/mL) was prepared in DMSO and freshly diluted with the assay buffer. Briefly, LNCaP cells (5×10^4) or PrEC cells (3×10^5) were seeded in six-well plates or T25 flasks and allowed to attach overnight. The cells were exposed to DMSO (control) or DATS as described above. Subsequently, the cells were collected by trypsinization and incubated for 15 min at 37°C in medium containing 10 μg/mL JC-1. The cells were washed with PBS, resuspended in 0.5 mL assay buffer, and analyzed using a Coulter Epics XL Flow Cytometer.

Protein Extraction and Immunoblotting

Cells (5×10^5) were seeded in 100-mm culture dishes, allowed to attach overnight, and exposed to DMSO (control) or desired concentrations of DATS for specified time periods. The cell lysate was prepared as described previously (15, 18, 19). The mitochondrial and cytosolic fractions from control and DATS-treated cells were prepared using a kit from BioVision according to the manufacturer's recommendations. Immunoblotting was done as described previously (15, 16, 18–20). Immunoreactive bands were visualized using the enhanced chemiluminescence method.

Immunocytochemical Analysis

Desired cells (1×10^5) were cultured on coverslips and treated with specified concentrations of DATS or DMSO (control) for the indicated time periods. Cells were stained with 200 nmol/L MitoTracker Red at 37°C for 30 min. After washing with PBS, the cells were fixed with 2% paraformaldehyde overnight at 4°C and permeabilized using 0.1% Triton X-100 in PBS for 10 min. The cells were washed with PBS, blocked with 2% bovine serum albumin in PBS for 1 h, and incubated with monoclonal anti–cytochrome *c* antibody or polyclonal anti-Smac/DIABLO, anti–Bcl-2 or anti–Bcl-xL antibody overnight at 4°C. The cells were washed with PBS, incubated with Alexa Fluor 488–conjugated secondary antibody (1:1,000 dilution, Molecular Probes) for 1 h at room temperature. Subsequently, the cells were washed with PBS and stained with DAPI (10 ng/mL) for 5 min at room temperature. The cells were washed twice with PBS and examined under a fluorescence microscope.

Transient Transfection of Bcl-2 and Bcl-xL

The LNCaP cells were transiently transfected with pSFFV–Bcl-2, pSFFV–Bcl-xL or pSFFV-neo plasmids generously provided by Dr. Stanley J. Korsmeyer (Dana-Farber Cancer Institute, Boston, MA). Briefly, the LNCaP cells were seeded in six-well plates and transfected at 60–70% confluency with pSFFV–Bcl-2, pSFFV–Bcl-xL or pSFFV-neo plasmid using FuGENE6 transfection reagent (Roche Applied Sciences) according to the manufacturer's instructions. The cells were cotransfected with pEGFP-N1 plasmid to determine transfection efficiency. Twenty-four hours after transfection, the cells were treated with DMSO or DATS for 24 h, collected, and processed for immunoblotting and immunocytochemistry to confirm overexpression and mitochondrial localization of Bcl-2 or Bcl-xL and analysis of cytoplasmic histone-associated DNA fragmentation.

RNA Interference of Bax and/or Bak

RNA interference of Bax was done using a Signal Silence Bax small interfering RNA (siRNA) purchased from Cell Signaling Technology. RNA interference of Bak was done using a Bak-targeted siRNA (Santa Cruz Biotechnology). A nonspecific control siRNA was purchased from Qiagen. LNCaP cells (1×10^4) were seeded in six-well plates and allowed to attach overnight. Cells were transfected with 100 nmol/L of desired siRNA using OligofectAMINE (Invitrogen) according to the manufacturer's recommendations. Twenty-four hours after transfection, cells were treated with DMSO (control) or desired concentrations of DATS for 24 h. Both floating and adherent cells were collected, washed with PBS, and processed for analysis of cytoplasmic histone-associated DNA fragmentation and immunoblotting.

Measurement of Intracellular ROS Generation

Intracellular ROS generation was measured by flow cytometry following staining with H_2DCFDA. Briefly, LNCaP cells (1×10^5 cells per well in six-well plates) or PrEC cells (3×10^5 cells/flask in T-25 flasks) were plated, allowed to attach overnight and exposed to DMSO (control) or desired concentrations of DATS for specified time periods. The cells were stained with 5 μmol/L H_2DCFDA for 30 min at 37°C, and the fluorescence was measured by flow cytometry as described previously (22). In some experiments, cells were either pretreated for 2 h with 4 mmol/L *N*-acetylcysteine and washed twice with PBS before DATS exposure or pretreated for 2 h with *N*-acetylcysteine and then cotreated with DATS.

Results

DATS Treatment Caused Apoptotic Cell Death in Human Prostate Cancer Cells Irrespective of Their Androgen Responsiveness

We have shown previously that DATS suppresses growth of androgen-independent PC-3 and DU145 human prostate cancer cells by causing apoptosis (15). However, it is unclear if the DATS-induced cell death is restricted to hormone-independent prostate cancer cells. In the present study, we addressed this question using an androgen-sensitive human prostate cancer cell line (LNCaP) and its androgen-independent variants LNCaP-C81 and LNCaP-C4-2. The C4-2 and C81 variants have been widely used to study the mechanism of prostate cancer progression from the androgen-responsive to androgen-independent state (23–26). The LNCaP-C4-2 cell line, which was generated through coculture of parental LNCaP cells with human bone fibroblasts *in vivo* in castrated male athymic mice, displays elevated prostate specific antigen expression and increased anchorage-independent growth in soft agar (27, 28). The LNCaP-C81 line was also derived from LNCaP cells through multiple passages in monolayer culture in RPMI 1640 supplemented with 5% FBS and 1% glutamine (29). As can be seen in Fig. 1A, DATS treatment caused an increase in fraction of apoptotic cells with condensed and fragmented DNA as judged by the DAPI assay. The DATS-induced apoptosis in LNCaP cells was confirmed by analysis of subdiploid fraction by flow cytometry (data not shown). Next, we compared sensitivities of parental LNCaP cells and its androgen-independent variants C81 (Fig. 1B) and C4-2 (data not shown) to DATS by trypan blue dye exclusion assay. Presence of 0.2% DMSO in the culture medium (solvent for DATS) did not have any appreciable effect on the viability of the cell lines examined in the present study (compare bars marked with the letters C and D in Fig. 1B representing untreated cells and cells treated with 0.2% DMSO, respectively). The viability of each cell line examined was decreased significantly in the presence of DATS in a concentration-dependent manner (Fig. 1B). Moreover, the cell-killing effect of DATS was more or less comparable between androgen-sensitive LNCaP cells and its androgen-refractory variants. Consistent with these results, DATS treatment caused a concentration-dependent and statistically significant increase in cytoplasmic histone-associated DNA fragmentation in LNCaP and LNCaP-C81 cells (Fig. 1C) as well as in LNCaP-C4-2 cells (data not shown). Interestingly, PrEC cell line, which has been used extensively as a representative normal prostate epithelial cell line (30, 31), was significantly more resistant to DATS-induced apoptosis even at 80 and 160 μmol/L concentrations (Fig. 1D). These results indicated that DATS selectively causes apoptosis in human prostate cancer cells irrespective of their androgen responsiveness.

DATS Treatment Caused Mitochondrial Membrane Potential Collapse

We have shown previously that DATS-induced apoptosis in PC-3 cells is significantly attenuated in the presence of a pan-caspase inhibitor and a caspase-9 specific inhibitor (19), suggesting the involvement of the mitochondrial pathway in the execution of apoptosis program (32, 33). To systematically explore this possibility, initially, we determined the effect of DATS treatment on mitochondrial morphology by transmission electron microscopy. Representative electron micrographs of LNCaP cells treated for 16 h with either DMSO (control) or 40 μmol/L DATS are depicted in Fig. 2A. The DMSO-treated control LNCaP cells exhibited a normal complement of healthy-looking mitochondria having an intact cristae structure. The mitochondria in DATS-treated cells seemed to have an intact outer membrane but disrupted cristae structure. The mitochondria of DATS-treated cells resembled type III mitochondria with intestinal or sausage-shape structure as described by Scorrano et al. (34). The DATS-mediated loss of the cristae structure was evident as early as 6 h posttreatment (data not shown).

We determined the effect of DATS treatment on mitochondrial membrane potential by flow cytometry following staining with a potential sensitive dye JC-1. The JC-1 dye bearing a delocalized positive charge enters the mitochondrial matrix due to the negative charge established by the intact mitochondrial membrane potential (35). In the absence of intact mitochondrial membrane potential, JC-1 accumulates in the cytoplasm in monomeric form characterized by green fluorescence (35). As can be seen in

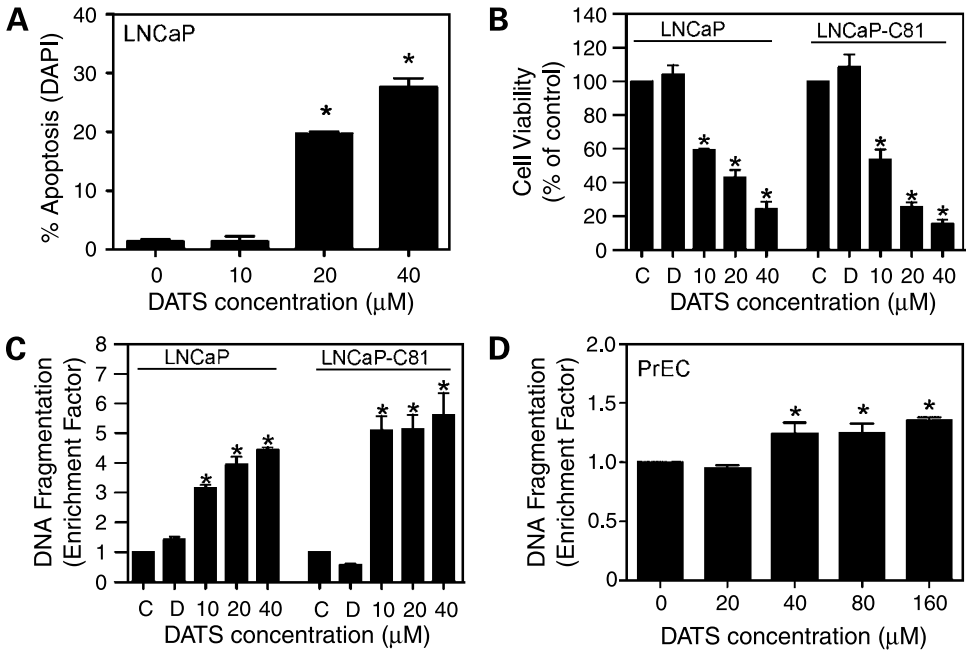

Figure 1. **A,** quantitation of apoptotic cells with condensed and fragmented DNA (DAPI assay) in LNCaP cultures treated for 24 h with either DMSO (control) or the indicated concentrations of DATS. *Columns,* mean ($n = 3$); *bars,* SE. *, $P < 0.05$, significantly different compared with DMSO-treated control by one-way ANOVA followed by Dunnett's test. **B,** effect of DATS treatment on the viability of LNCaP and LNCaP-C81 cells as determined by trypan blue dye exclusion assay. Desired cell line was either untreated (*C*) or treated with DMSO (final concentration 0.2%; *D*) or the indicated concentrations of DATS for 24 h and then processed for trypan blue dye exclusion assay. **C,** cytoplasmic histone-associated DNA fragmentation in cultures of control and DATS-treated LNCaP and LNCaP-C81 cells. Desired cell line was either untreated (*C*) or treated with DMSO (final concentration 0.2%; *D*) or the indicated concentrations of DATS for 24 h and then processed for cytoplasmic histone-associated DNA fragmentation assay. The enrichment factor relative to untreated control was calculated as recommended by the manufacturer. **D,** cytoplasmic histone-associated DNA fragmentation in PrEC normal prostate epithelial cells following 24 h exposure to DMSO or the indicated concentrations of DATS. The enrichment factor relative to DMSO-treated control is shown. In (**B**–**D**), *columns,* mean ($n = 3$); *bars,* SE. *, significantly different compared with either untreated control (**B** and **C**) or DMSO-treated control (**D**). Similar results were observed in at least two independent experiments.

Fig. 2B, the DMSO-treated control LNCaP cells predominantly exhibited red fluorescence with minimal green fluorescence, indicating intact mitochondrial membrane potential. The DATS treatment caused a time-dependent and statistically significant increase in the percentage of cells with green fluorescence, indicating collapse of the mitochondrial membrane potential, which was evident as early as 1 h posttreatment (Fig. 2B). In dose-response studies, after 2 h treatment, the DATS-mediated collapse of the mitochondrial membrane potential was observed at 10 and 20 μmol/L concentrations (data not shown). Interestingly, the PrEC cell line was resistant to the DATS-mediated disruption of the mitochondrial membrane potential at least for up to 6 h of treatment with 20 and 40 μmol/L DATS (Fig. 2C).

To test whether DATS-mediated disruption of the mitochondrial membrane potential was accompanied by cytosolic release of apoptogenic molecules, mitochondrial and cytosolic fractions were prepared from control and DATS-treated cells and subjected to immunoblotting for cytochrome *c*. As shown in Fig. 2D, treatment of LNCaP cells with 10, 20, and 40 μmol/L DATS for 8 h resulted in an increase in cytosolic level of cytochrome *c*, which was accompanied by a decrease in its level in the mitochondria. The blot was stripped and reprobed with anti-COX IV and anti-actin antibodies to ensure equal protein loading as well as to rule out cross-contamination of mitochondrial and cytosolic fractions. The DATS-mediated release of apoptogenic molecules from the mitochondria to the cytosol was also evident in the immunohistochemical analysis of cytochrome *c* and Smac/DIABLO (data not shown). Collectively, these results indicated that DATS-induced apoptosis in our model was accompanied by the collapse of the mitochondrial membrane potential and the translocation of apoptogenic molecules from the mitochondria to the cytosol.

Effect of DATS Treatment on Levels of Bcl-2 Family Proteins

The Bcl-2 family proteins have emerged as critical regulators of mitochondria-mediated apoptosis by functioning as either promoters (e.g., Bax and Bak) or inhibitors (e.g., Bcl-2 and Bcl-xL) of the cell death process (36). Because DATS treatment disrupted mitochondrial membrane potential leading to cytosolic release of apoptogenic molecules in LNCaP cells, we proceeded to test whether DATS-induced apoptosis was regulated by Bcl-2 family proteins. We determined the effect of DATS treatment on levels of Bcl-2 family proteins in LNCaP cells by immunoblotting,

and representative blots are shown in Fig. 3A. The levels of antiapoptotic proteins Bcl-2 and Bcl-xL were decreased on treatment of LNCaP cells with DATS. In addition, DATS treatment resulted in a modest increase in levels of multidomain proapoptotic protein Bak. The DATS-mediated induction of Bak protein was evident as early as 2 h after treatment and was sustained for the duration of the experiment (Fig. 3A). The DATS treatment did not have any appreciable effect on Bid protein level (Fig. 3A). Figure 3B summarizes the effect of DATS treatment on Bax and Bak protein levels in PrEC cells. Expression of Bax or Bak proteins was not altered by treatment of PrEC cells with 40 μmol/L DATS for 4, 8, 16, or 24 h (Fig. 3B). These results indicated that DATS treatment altered the ratio of proapoptotic to antiapoptotic Bcl-2 family proteins in LNCaP cells.

Because DATS treatment caused a decrease in protein level of Bcl-2, we determined the effect of its overexpression on DATS-induced apoptosis. The LNCaP cells transiently transfected with the empty vector (hereafter abbreviated as LNCaP/Neo) were used as control for direct comparison. The cells were cotransfected with pEGFP-N1 plasmid to determine transfection efficiency, which varied between 50% and 70% in different transfection experiments. Overexpression of Bcl-2 in LNCaP cells transfected with pSFFV–Bcl-2 plasmid (hereafter abbreviated as LNCaP/Bcl-2 cells) was confirmed by immunoblotting. The level of Bcl-2 protein was markedly higher in LNCaP/Bcl-2 cells than in LNCaP/Neo cells (Fig. 4A). Immunocytochemical analysis confirmed the mitochondrial localization of Bcl-2 in LNCaP/Bcl-2 cells (data not shown). Interestingly, the LNCaP/Neo and LNCaP/Bcl-2 cells were equally sensitive toward DATS-induced cytoplasmic histone-associated DNA fragmentation (Fig. 4B). These results indicated that the DATS-induced apoptosis in LNCaP cells was probably not attributable to the down-regulation of Bcl-2.

Next, we determined the effect of ectopic expression of Bcl-xL, which is a Bcl-2 homologue and functions to inhibit cell death by different stimuli (36). The level of Bcl-xL

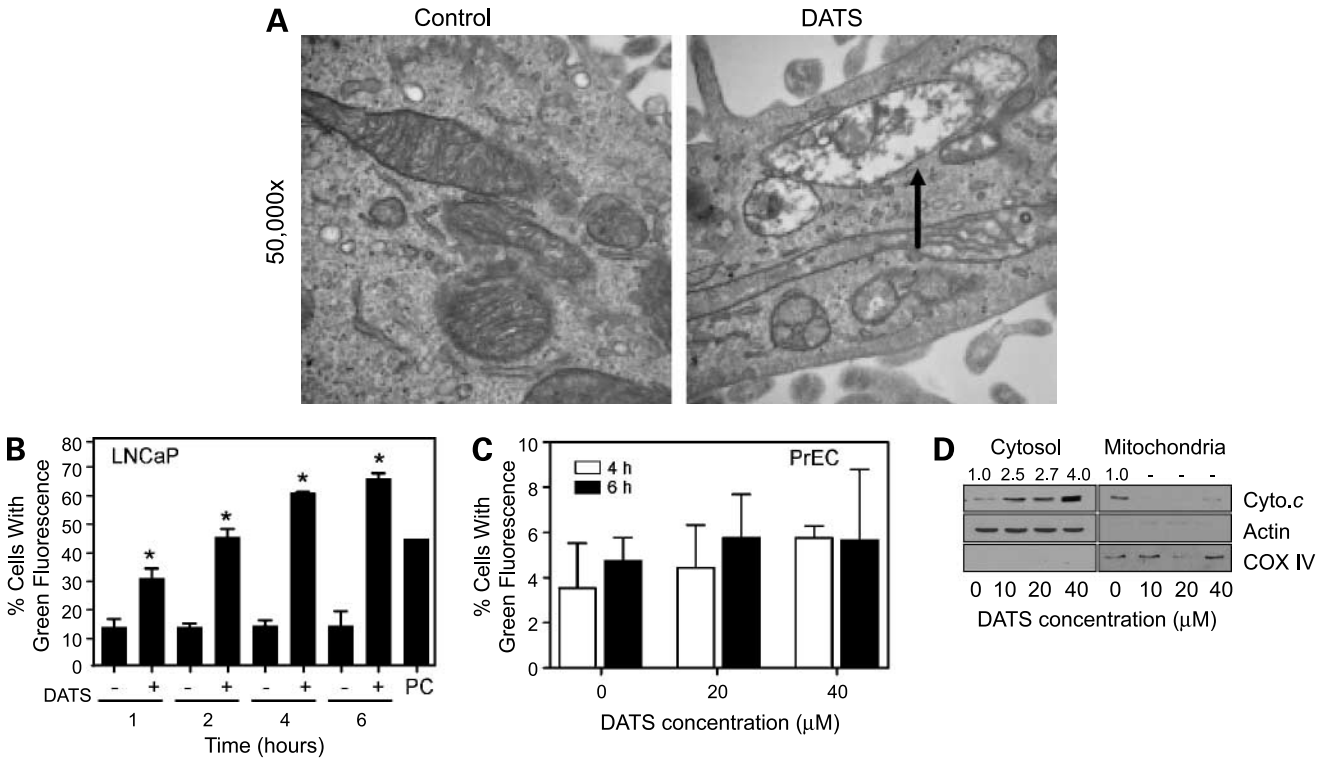

Figure 2. **A,** representative transmission electron micrographs of LNCaP cell following 16 h treatment with DMSO (control) or 40 μmol/L DATS (magnification, ×50,000). Note control LNCaP cells exhibited healthy-looking mitochondria having an intact cristae structure. The DATS treatment caused disruption of mitochondrial cristae structure (*arrow*), and a large fraction of mitochondria in DATS-treated cells resembled type III mitochondria (34). **B,** percentage of cells with cytosolic monomeric JC-1–associated green fluorescence (indicating collapse of mitochondrial membrane potential) in LNCaP cultures treated with DMSO (control) or 40 μmol/L DATS for the indicated time periods. The LNCaP cells treated for 30 min with 25 μmol/L FCCP were included as a positive control (*PC*). Representative data from a single experiment (mean ± SE, $n = 3$), which was repeated with similar results, are shown. *, $P < 0.05$, significantly different compared with corresponding DMSO-treated control by paired t test. **C,** percentage of cells with cytosolic monomeric JC-1–associated green fluorescence in PrEC cultures treated with DMSO (control) or the indicated concentrations of DATS for 4 or 6 h. *Columns,* mean ($n = 2–3$); *bars,* SE. **D,** immunoblotting for cytochrome *c* using cytosolic and mitochondrial fractions prepared from LNCaP cells following 8 h treatment with DMSO (control) or the indicated concentrations of DATS. The blots were stripped and reprobed with anti-actin and anti-COX IV antibodies to ensure equal protein loading as well as to rule out cross-contamination of mitochondrial and cytosolic fractions. Densitometric scanning data after correction for actin loading control are shown on top of each band. Immunoblotting was done twice using independently prepared lysates, and the results were comparable.

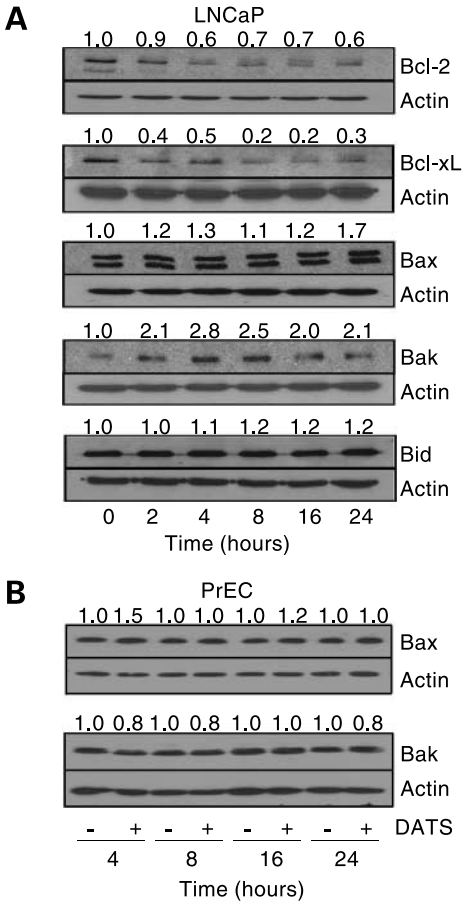

Figure 3. **A,** immunoblotting for Bcl-2, Bcl-xL, Bax, Bak, and Bid using lysates from LNCaP cells treated with 40 μmol/L DATS for the indicated time periods. **B,** immunoblotting for Bax and Bak using lysates from PrEC cells treated with DMSO (control) or 40 μmol/L DATS for the indicated time periods. The blots were stripped and reprobed with anti-actin antibody to normalize for differences in protein loading. Densitometric scanning data after correction for actin loading control are shown on top of each band. Immunoblotting for each protein was done at least twice using independently prepared lysates.

protein was markedly higher in LNCaP cells transiently transfected with pSFFV–Bcl-xL plasmid (LNCaP/Bcl-xL cells) than in the empty vector-transfected control LNCaP/Neo cells (Fig. 4C). The DATS-induced cytoplasmic histone-associated DNA fragmentation was evident not only in vector-transfected control cells but also in LNCaP/Bcl-xL cells (Fig. 4D). Moreover, the cytoplasmic histone-associated DNA fragmentation resulting from a 24-h treatment with 40 μmol/L DATS did not differ significantly between LNCaP/Neo and LNCaP/Bcl-xL cells as judged by paired *t* test (Fig. 4D). Collectively, these results indicated that DATS-induced apoptosis in LNCaP cells was not influenced by Bcl-2 or Bcl-xL protein level.

Bak and Bax Knockdown Conferred Significant Protection against DATS-Induced Apoptosis

Because DATS treatment caused an increase in the protein level of Bak (Fig. 3A), we hypothesized that this protein might play an important role in the regulation of DATS-induced apoptosis. We tested this hypothesis by comparing sensitivities of SV40-immortalized MEFs derived from WT and DKO mice toward DATS-induced apoptosis. Because of immortalization by transfection with SV40 genomic DNA, the MEFs cannot be regarded as normal fibroblasts. Initially, we used the MEFs from WT mice to determine the effect of DATS treatment on levels of Bak and Bax proteins. Similar to LNCaP cells, DATS treatment resulted in a modest induction of Bax and Bak protein levels in WT MEFs (data not shown). The DATS treatment caused concentration-dependent and statistically significant increase in apoptotic cells in WT MEFs as judged by the analysis of cytoplasmic histone-associated DNA fragmentation (Fig. 5A) and subdiploid fraction (data not shown). On the other hand, the MEFs derived from DKO MEFs mice were significantly more resistant to DATS-induced cytoplasmic histone-associated DNA fragmentation compared with WT MEFs (Fig. 5A). To test whether Bak and Bax proteins function upstream of cytosolic release of cytochrome *c* in our model, we determined the effect of DATS treatment on cytosolic release of cytochrome *c* using WT and DKO MEFs. As can be seen in Fig. 5B, the DATS-mediated cytosolic release of cytochrome *c* was approximately 2-fold higher in WT MEFs compared with DKO. Consistent with these results, DATS treatment caused proteolytic cleavage of procaspase-3 in WT MEFs as evidenced by the appearance of a 17-kDa cleaved intermediate, which was barely detectable in DKO even after DATS treatment (Fig. 5B). Collectively, these results indicated that Bax and Bak play an important role in the execution of DATS-induced apoptosis.

We used Bax- and Bak-targeted siRNA to confirm the involvement of these proteins in the regulation of DATS-induced apoptosis. As can be seen in Fig. 5C, the level of Bax protein was decreased by about 65% in LNCaP cells transiently transfected with Bax siRNA. Although transfection of LNCaP cells with the Bax-targeted siRNA also resulted in a marked decrease in protein level of Bak, the Bak-targeted siRNA was more specific and caused the knockdown of only Bak. Nonetheless, the cytoplasmic histone-associated DNA fragmentation resulting from a 24-h treatment with 20 and 40 μmol/L DATS was statistically significantly lower in LNCaP cells with combined knockdown of Bax and Bak proteins compared with cells transiently transfected with a control nonspecific siRNA (Fig. 5D). Together, these results indicated that Bax and Bak were targets of DATS-induced cell death.

DATS-Induced Apoptosis in LNCaP Cells Correlated with ROS Generation

ROS are implicated in apoptosis induction by different stimuli including ionizing radiation and hyperoxia (37, 38). We have shown previously that DATS-mediated G_2-M phase cell cycle arrest in PC-3 and DU145 cells correlates with ROS generation (16). We designed experiments to determine whether DATS-induced apoptosis was mediated by ROS. Intracellular ROS generation in control (DMSO treated) and DATS-treated LNCaP cells was assessed by

flow cytometry following staining with H_2DCFDA (22). The H_2DCFDA is cleaved by nonspecific cellular esterases and oxidized in the presence of H_2O_2 and other peroxides to yield fluorescent 2′,7′-dichlorofluorescein (DCF). The DATS-treated LNCaP cells exhibited a concentration-dependent and statistically significant increase in DCF fluorescence (Fig. 6A), which was significantly attenuated by a 2-h pretreatment with antioxidant *N*-acetylcysteine (Fig. 6B). Moreover, *N*-acetylcysteine pretreatment conferred near-complete protection against DATS-induced disruption of the mitochondrial membrane potential (Fig. 6C) and cytoplasmic histone-associated DNA fragmentation (Fig. 6D). Interestingly, ROS generation was not observed in PrEC cells treated with 40 μmol/L DATS for at least up to 16 h (data not shown). The *N*-acetylcysteine–mediated protection against DATS-induced apoptosis was maintained even if the cells were washed twice with PBS and suspended in *N*-acetylcysteine–free media before DATS exposure (data not shown). Together, these results indicated that DATS-induced apoptosis in LNCaP cells correlated with ROS generation.

Discussion

Prostate cancer is a leading cause of cancer-related deaths among men in the United States. Because the majority of the prostate cancers are androgen dependent at the time of diagnosis, hormone withdrawal is a frequently prescribed treatment option for initial management of this malignancy (39). This treatment modality, however, is palliative and has limited scope for hormone-refractory prostate cancers, which are highly aggressive and metastatic (39). Chemotherapy and radiation therapy are largely ineffective against hormone-independent prostate cancer (40, 41). Prostate cancer is usually diagnosed in the sixth and seventh decades of life, which presents a large window of opportunity for intervention to prevent or slow progression of the disease. Therefore, clinical development of agents that are nontoxic to normal cells but can inhibit growth of both hormone-responsive and hormone-independent prostate cancers could have a significant impact on disease-related cost, morbidity, and mortality for a large segment of the population. The results of the present study indicate that DATS meets all these criteria. First, DATS inhibits proliferation of androgen-sensitive LNCaP cells and its androgen-independent variants (LNCaP-C81 and LNCaP-C4-2) by causing apoptosis. Second, the PrEC normal prostate epithelial cell line is significantly more resistant to growth inhibition and apoptosis induction by DATS even at concentrations that are highly cytotoxic to the prostate cancer cells. Third, we have shown recently that oral administration of DATS (6 μmol, thrice per week) significantly retards growth of PC-3 xenografts *in vivo* in athymic mice in association with apoptotic cell death (42).

The DATS-mediated cell growth arrest and apoptosis induction in human prostate cancer cells (refs. 15, 16, 18, 19 and the present study) is evident at concentrations (10–40 μmol/L) that are well within the pharmacologically

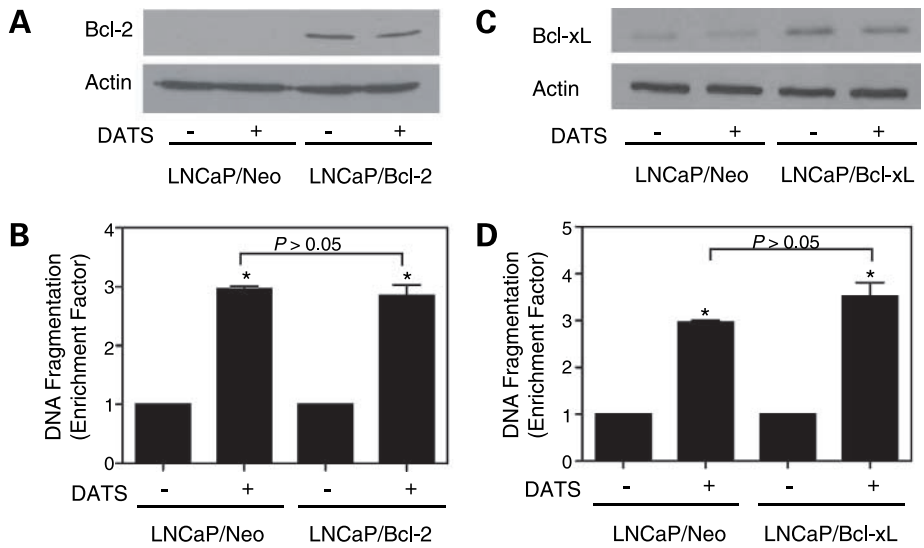

Figure 4. **A,** immunoblotting for Bcl-2 protein using lysates from LNCaP cells transiently transfected with empty vector (LNCaP/Neo cells) or pSFFV–Bcl-2 plasmid (LNCaP/Bcl-2 cells) and treated for 24 h with either DMSO (control) or 40 μmol/L DATS. The blot was stripped and reprobed with anti-actin antibody to ensure equal protein loading. **B,** cytoplasmic histone-associated DNA fragmentation in LNCaP/Neo and LNCaP/Bcl-2 cells following 24 h treatment with DMSO (control) or 40 μmol/L DATS. **C,** immunoblotting for Bcl-xL protein using lysates from LNCaP cells transiently transfected with empty vector (LNCaP/Neo cells) or pSFFV–Bcl-xL plasmid (LNCaP/Bcl-xL cells) and treated for 24 h with either DMSO (control) or 40 μmol/L DATS. The blot was stripped and reprobed with anti-actin antibody to ensure equal protein loading. **D,** cytoplasmic histone-associated DNA fragmentation in LNCaP/Neo and LNCaP/Bcl-xL cells following 24 h treatment with DMSO (control) or 40 μmol/L DATS. In (**B** and **D**), *columns,* mean ($n = 3$); *bars,* SE. *, $P < 0.05$, significantly different compared with corresponding DMSO treated control by one-way ANOVA followed by Bonferroni's multiple comparison test. Similar results were observed in replicate experiments.

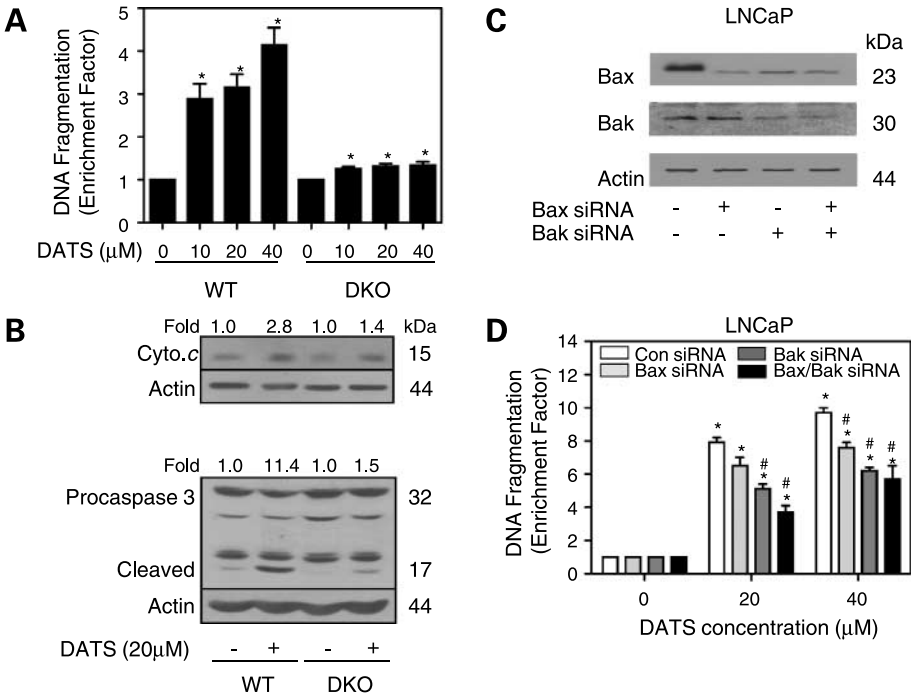

Figure 5. **A,** cytoplasmic histone-associated DNA fragmentation in MEFs derived from WT or DKO mice following 24 h treatment with DMSO or the indicated concentrations of DATS. *Columns,* mean ($n = 3$); *bars,* SE. *, $P < 0.05$, significantly different compared with corresponding DMSO-treated control by one-way ANOVA followed by Dunnett's test. **B,** immunoblotting for cytochrome *c* and procaspase-3 using lysates from MEFs derived from WT or DKO mice treated for 16 h with 20 μmol/L DATS. The blots were stripped and reprobed with anti-actin antibody to ensure equal protein loading. Densitometric scanning data after correction for actin loading control are shown on top of each band. **C,** immunoblotting for Bax and Bak using lysates from LNCaP cells transiently transfected with a nonspecific control siRNA and Bax and/or Bak-targeted siRNA. The blot was stripped and reprobed with anti-actin antibody to ensure equal protein loading. **D,** cytoplasmic histone-associated DNA fragmentation in LNCaP cells transiently transfected with a control siRNA or Bax and/or Bak siRNA and treated for 24 h with either DMSO (control) or the indicated concentrations of DATS. *Columns,* mean ($n = 3$); *bars,* SE. *, $P < 0.05$, significantly different compared with corresponding DMSO-treated control by one-way ANOVA followed by Dunnett's test; #, significantly different between DATS-treated control siRNA and DATS-treated Bax and/or Bak siRNA groups by paired *t* test. Similar results were observed in at least two independent experiments.

achievable range based on a recent pharmacokinetic study (43). The peak plasma concentration of DATS in rats following treatment with 10 mg DATS was shown to be about 31 μmol/L (43). Although the pharmacokinetic parameters for DATS in humans have not yet been measured, oral administration of 200 mg of synthetic DATS (also known as allitridum) in combination with 100 μg selenium every other day for 1 month to humans did not cause any harmful side effects (44). It is therefore possible that the plasma concentrations of DATS required for cancer cell growth inhibition may be achievable in humans.

The present study indicates that the DATS-mediated apoptosis in LNCaP cells is accompanied by morphologic changes in mitochondria and the collapse of the mitochondrial membrane potential, leading to the release of apoptogenic molecules from the mitochondria to the cytosol. Interestingly, the DATS-mediated disruption of the mitochondrial membrane potential is not observed in PrEC cells. To the best of our knowledge, the present study is the first published report to show the involvement of the mitochondria in the execution of DATS-induced apoptosis. Antiapoptotic Bcl-2 family members (Bcl-2 and Bcl-xL) play an important role in the regulation of mitochondria-mediated apoptosis by different stimuli (36). The anti-apoptotic Bcl-2 family members possess four conserved Bcl-2 homology domains (BH1-BH4) and mainly prevent the release of apoptogenic molecules (e.g., cytochrome *c*) from mitochondria to the cytosol by forming heterodimer complexes with proapoptotic family members such as Bax (36, 45, 46). Increased expression of Bcl-2 has been observed in a variety of hematologic malignancies and solid tumors, and overexpression of Bcl-2 renders cancer cells resistant to different apoptotic stimuli including chemotherapeutic agents (47). The DATS treatment causes a decrease in protein levels of both Bcl-2 and Bcl-xL in LNCaP cells. It is interesting to note, however, that the ectopic expression of either Bcl-2 or Bcl-xL fails to confer significant protection against DATS-induced cell death in LNCaP cells. Thus, DATS can overcome the antiapoptotic actions of Bcl-2 and Bcl-xL and promote apoptosis even in cells that over-express these important oncoproteins.

The proapoptotic Bcl-2 family proteins, which can be subdivided into the Bax subfamily of multidomain proteins (e.g., Bax and Bak) or BH3-only subfamily (e.g., Bid), induce mitochondrial membrane permeabilization and release of apoptogenic molecules from mitochondria to

the cytosol (36, 45, 46). The present study indicates that Bax and Bak proteins play an important role in the regulation of DATS-induced apoptosis because (*a*) the SV40-immortalized MEFs derived from DKO mice are significantly more resistant toward DATS-induced cell death compared with the WT MEFs; (*b*) the DATS-mediated cytosolic release of cytochrome *c* and cleavage of procaspase-3 is relatively more pronounced in the MEFs derived from WT mice than in the MEFs derived from DKO mice; and (*c*) Bax and Bak knockdown in LNCaP cells confers statistically significant protection against DATS-induced apoptosis. We have shown recently that the DATS-mediated inhibition of PC-3 xenograft growth in athymic mice *in vivo* correlates not only with increased apoptosis but also induction of Bax and Bak proteins in the tumor tissues (42). It is important to point out, however, that Bax and Bak cannot fully explain the cell death caused by DATS because combined knockdown of these proteins confers only partial protection against DATS-induced apoptosis. It is intriguing to note that DATS treatment causes only a modest increase in protein levels of Bax and Bak, yet knockdown of these proteins confers statistically significant protection against DATS-induced apoptosis. Although the precise mechanism by which Bax and Bak regulate DATS-induced cell death remains elusive, it is possible that DATS treatment causes conformation change and oligomerization of Bax/Bak leading to their translocation to the mitochondria. This possibility is likely based on following considerations: (*a*) Bax activation by certain apoptotic stimuli is dependent on ROS generation (38), which is observed in DATS-treated prostate cancer cells (present study), and (*b*) microtubule-damaging agents have been shown to cause Bax activation (48), and DATS treatment is known to disrupt tubulin network (18). However, further studies are needed to systematically explore this possibility.

The DATS-induced cell death in LNCaP cells correlates with ROS generation. Because ROS generation is implicated in the pathogenesis of many chronic diseases including cancer, the potential side effects of DATS-mediated ROS production cannot be ignored. However, we are tempted to speculate that ROS generation by DATS may not be deleterious because (*a*) DATS is derived from vegetables consumed by humans on a daily basis, yet epidemiologic studies continue to support the premise that dietary intake

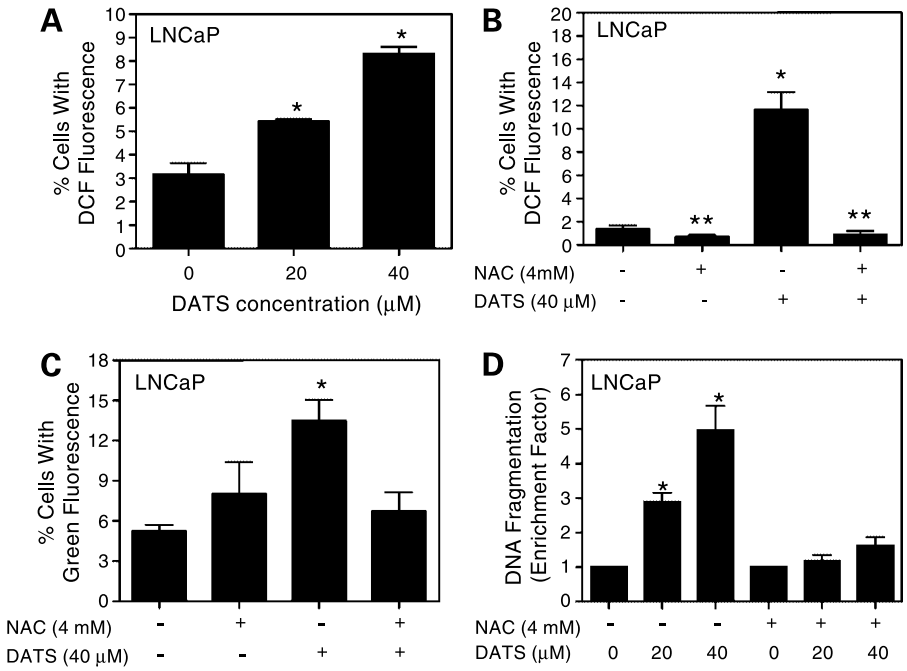

Figure 6. **A,** percentage of DCF-positive cells (a measure of ROS generation) in LNCaP cultures following 8 h treatment with DMSO (control) or the indicated concentrations of DATS. *Columns,* mean ($n = 4$); *bars,* SE. *, $P < 0.05$, significantly different compared with DMSO-treated control by one-way ANOVA followed by Dunnett's test. **B,** percentage of DCF-positive cells in LNCaP cultures treated for 8 h with DMSO (control) or 40 μmol/L DATS in the absence or presence of 4 mmol/L *N*-acetylcysteine (2 h pretreatment). *Columns,* mean ($n = 3$); *bars,* SE. *, $P < 0.05$, significantly different compared with DMSO-treated control; **, $P < 0.05$, significantly different compared with DATS treatment group by one-way ANOVA followed by Bonferroni's multiple comparison test. **C,** percentage of cells with cytosolic accumulation of monomeric JC-1 (green fluorescence) in LNCaP cultures treated for 6 h with DMSO (control) or 40 μmol/L DATS in the absence or presence of 4 mmol/L *N*-acetylcysteine (2 h pretreatment). *Columns,* mean ($n = 3$); *bars,* SE. *, $P < 0.05$, significantly different compared with DMSO-treated control by one-way ANOVA followed by Bonferroni's multiple comparison test. **D,** cytoplasmic histone-associated DNA fragmentation in LNCaP cultures following 24 h treatment with DMSO (control) or the indicated concentrations of DATS in the absence or presence of 4 mmol/L *N*-acetylcysteine (2 h pretreatment). *Columns,* mean ($n = 3$); *bars,* SE. *, $P < 0.05$, significantly different compared with the corresponding DMSO-treated control by one-way ANOVA followed by Bonferroni's multiple comparison test. The enrichment factor was statistically significantly lower ($P < 0.05$) in *N*-acetylcysteine pretreated cells than in cells without *N*-acetylcysteine treatment at both 20 and 40 μmol/L DATS concentrations. Each experiment was done at least twice, and representative data from a single experiment are shown.

of *Allium* vegetables including garlic may reduce the risk of different types of malignancies, including cancer of the prostate (1–3); (*b*) the DATS-treated athymic mice do not exhibit weight loss or any other signs of toxicity (42); and (*c*) a normal prostate epithelial cell line (PrEC) seems resistant to DATS-mediated ROS generation, mitochondrial membrane potential collapse, and apoptosis induction (present study). It is possible that the DATS-mediated ROS generation in cancer cells is transient and serves to trigger the apoptosis signaling cascade.

In conclusion, the present study reveals that DATS causes apoptosis in human prostate cancer cells, but not in a normal prostate epithelial cell line (PrEC), which correlates with mitochondrial membrane potential collapse and ROS generation. The DATS-induced cell death is regulated by Bax/Bak but independent of Bcl-2 and Bcl-xL.

Acknowledgments

We thank Dr. Stanley J. Korsmeyer for the generous gifts of pSFFV – Bcl-2, pSFFV – Bcl-xL, and pSFFV-neo plasmids and the MEFs derived from WT, Bax, and/or Bak knock-out mice and Dr. Ming-Fong Lin for the generous gift of LNCaP-C81 cells.

References

1. You WC, Blot WJ, Chang YS, et al. Allium vegetables and reduced risk of stomach cancer. J Natl Cancer Inst 1989;18:162 – 4.

2. Gao CM, Takezaki T, Ding JH, Li MS, Tajima K. Protective effect of allium vegetables against both esophageal and stomach cancer: a simultaneous case-referent study of a high-epidemic area in Jiangsu Province, China. Jpn J Cancer Res 1999;90:614 – 21.

3. Hsing AW, Chokkalingam AP, Gao YT, et al. Allium vegetables and risk of prostate cancer: a population-based study. J Natl Cancer Inst 2002;94: 1648 – 51.

4. Block E. The organosulfur chemistry of the genus *Allium* — implications for the organic chemistry of sulfur. Angew Chem Int Ed Engl 1992;31: 1135 – 78.

5. Sparnins VL, Barany G, Wattenberg LW. Effects of organosulfur compounds from garlic and onions on benzo(*a*)pyrene-induced neoplasia and glutathione *S*-transferase activity in the mouse. Carcinogenesis 1988; 9:131 – 4.

6. Wargovich MJ, Woods C, Eng VWS, Stephens LC, Gray K. Chemoprevention of *N*-nitrosomethylbenzylamine – induced esophageal cancer in rats by the naturally occurring thioether, diallyl sulfide. Cancer Res 1988; 48:6872 – 5.

7. Reddy BS, Rao CV, Rivenson A, Kelloff G. Chemoprevention of colon carcinogenesis by organosulfur compounds. Cancer Res 1993;53: 3493 – 8.

8. Hu X, Benson PJ, Srivastava SK, et al. Induction of glutathione S-transferase π as a bioassay for the evaluation of potency of inhibitors of benzo(*a*)pyrene-induced cancer in a murine model. Int J Cancer 1997;73: 897 – 902.

9. Singh SV, Pan SS, Srivastava SK, et al. Differential induction of NAD(P)H:quinone oxidoreductase by anti-carcinogenic organosulfides from garlic. Biochem Biophys Res Commun 1998;244:917 – 20.

10. Brady JF, Ishizaki H, Fukuto JM, et al. Inhibition of cytochrome P-450 2E1 by diallyl sulfide and its metabolites. Chem Res Toxicol 1991; 4:642 – 7.

11. Singh SV. Impact of garlic organosulfides on p21(H-ras) processing. J Nutr 2001;131:1046 – 8s.

12. Sundaram SG, Milner JA. Diallyl disulfide induces apoptosis of human colon tumor cells. Carcinogenesis 1996;17:669 – 73.

13. Knowles LM, Milner JA. Diallyl disulfide inhibits p34(cdc2) kinase activity through changes in complex formation and phosphorylation. Carcinogenesis 2000;21:1129 – 34.

14. Nakagawa H, Tsuta K, Kiuchi K, et al. Growth inhibitory effects of diallyl disulfide on human breast cancer cell lines. Carcinogenesis 2001; 22:891 – 7.

15. Xiao D, Choi S, Johnson DE, et al. Diallyl trisulfide-induced apoptosis in human prostate cancer cells involves c-Jun N-terminal kinase and extracellular-signal regulated kinase-mediated phosphorylation of Bcl-2. Oncogene 2004;23:5594 – 606.

16. Xiao D, Herman-Antosiewicz A, Antosiewicz J, et al. Diallyl trisulfide-induced G_2-M phase cell cycle arrest in human prostate cancer cells is caused by reactive oxygen species-dependent destruction and hyperphosphorylation of Cdc25C. Oncogene 2005;24:6256 – 68.

17. Hosono T, Fukao T, Ogihara J, et al. Diallyl trisulfide suppresses the proliferation and induces apoptosis of human colon cancer cells through oxidative modification of β-tubulin. J Biol Chem 2005;280:41487 – 93.

18. Herman-Antosiewicz A, Singh SV. Checkpoint kinase 1 regulates diallyl trisulfide – induced mitotic arrest in human prostate cancer cells. J Biol Chem 2005;280:28519 – 28.

19. Xiao D, Singh SV. Diallyl trisulfide, a constituent of processed garlic, inactivates Akt to trigger mitochondrial translocation of BAD and caspase-mediated apoptosis in human prostate cancer cells. Carcinogenesis 2006; 27:533 – 40.

20. Antosiewicz J, Herman-Antosiewicz A, Marynowski SW, Singh SV. c-Jun NH_2-terminal kinase signaling axis regulates diallyl trisulfide-induced generation of reactive oxygen species and cell cycle arrest in human prostate cancer cells. Cancer Res 2006;66:5379 – 86.

21. Wei MC, Zong WX, Cheng EH, et al. Proapoptotic Bax and Bak: a requisite gateway to mitochondrial dysfunction and death. Science 2001; 292:727 – 30.

22. Singh SV, Srivastava SK, Choi S, et al. Sulforaphane-induced cell death in human prostate cancer cells is initiated by reactive oxygen species. J Biol Chem 2005;280:19911 – 24.

23. Karan D, Schmied BM, Dave BJ, Wittel UA, Lin MF, Batra SK. Decreased androgen-responsive growth of human prostate cancer is associated with increased genetic alterations. Clin Cancer Res 2001;7: 3472 – 80.

24. Karan D, Kelly DL, Rizzino A, Lin MF, Batra SK. Expression profile of differentially-regulated genes during progression of androgen-independent growth in human prostate cancer cells. Carcinogenesis 2002;23:967 – 75.

25. Oudes AJ, Roach JC, Walashek LS, et al. Application of Affymetrix array and Massively Parallel Signature Sequencing for identification of genes involved in prostate cancer progression. BMC Cancer 2005;5:86.

26. Saporita AJ, Ai J, Wang Z. The Hsp90 inhibitor, 17-AAG, prevents the ligand-independent nuclear localization of androgen receptor in refractory prostate cancer cells. Prostate 2007;67:509 – 20.

27. Thalmann GN, Anezinis PE, Chang SM, et al. Androgen-independent cancer progression and bone metastasis in the LNCaP model of human prostate cancer. Cancer Res 1994;54:2577 – 81.

28. Wu HC, Hsieh JT, Gleave ME, Brown NM, Pathak S, Chung LW. Derivation of androgen-independent human LNCaP prostatic cancer cell sublines: role of bone stromal cells. Int J Cancer 1994;57:406 – 12.

29. Igawa T, Lin FF, Lee MS, Karan D, Batra SK, Lin MF. Establishment and characterization of androgen-independent human prostate cancer LNCaP cell model. Prostate 2002;50:222 – 35.

30. Campbell CL, Savarese DMF, Quesenberry PJ, Savarese TM. Expression of multiple angiogenic cytokines in cultured normal human prostate epithelial cells: predominance of vascular endothelial growth factor. Int J Cancer 1999;80:868 – 74.

31. Chen L, Hodge GB, Guarda LA, Welch JL, Greenberg NM, Chai KX. Down-regulation of prostasin serine protease: a potential invasion suppressor in prostate cancer. Prostate 2001;48:93 – 103.

32. Thornberry N, Lazebnick Y. Caspases: enemies within. Science 1998; 281:1312 – 6.

33. Wolf BB, Green DR. Suicidal tendencies: apoptotic cell death by caspase family proteinases. J Biol Chem 1999;274:20049 – 52.

34. Scorrano L, Ashiya M, Buttle K, et al. A distinct pathway remodels mitochondrial cristae and mobilizes cytochrome *c* during apoptosis. Dev Cell 2002;2:55 – 67.

35. Cossarizza A, Baccarani-Contri M, Kalashnikova G, Franceschi C. A new method for the cytofluorimetric analysis of mitochondrial membrane potentials using the J-aggregate forming lipophilic cation 5,5′,6,6′-tetrachloro-1,1′,3,3′-tetraethylbenzimidazolylcarbocyanine iodide (JC-1). Biochem Biophys Res Commun 1993;197:40 – 5.

36. Chao DT, Korsmeyer SJ. BCL-2 family: regulators of cell death. Annu Rev Immunol 1998;16:395 – 419.

37. Leach JK, Van Tuyle G, Lin PS, Schmidt-Ullrich R, Mikkelsen RB.

Ionizing radiation-induced, mitochondria-dependent generation of reactive oxygen/nitrogen. Cancer Res 2001;61:3894 – 901.

38. Buccellato LJ, Tso M, Akinci OI, Chandel NS, Budinger GR. Reactive oxygen species are required for hyperoxia-induced Bax activation and cell death in alveolar epithelial cells. J Biol Chem 2004;279:6753 – 60.

39. Laufer M, Denmeade SR, Sinibaldi VJ, Carducci MA, Eisenberger MA. Complete androgen blockade for prostate cancer: what went wrong? J Urol 2000;164:3 – 9.

40. Stein ME, Boehmer D, Kuten A. Radiation therapy in prostate cancer. Recent Results Cancer Res 2007;175:179 – 99.

41. Gilligan T, Kantoff PW. Chemotherapy for prostate cancer. Urol 2002; 60:94 – 100.

42. Xiao D, Lew KL, Kim Y, et al. Diallyl trisulfide suppresses growth of PC-3 human prostate cancer xenograft *in vivo* in association with Bax and Bak induction. Clin Cancer Res 2006;12:6836 – 43.

43. Sun X, Guo T, He J, et al. Determination of the concentration of diallyl trisulfide in rat whole blood using gas chromatography with electron-capture detection and identification of its major metabolite with gas chromatography mass spectrometry. Yakugaku Zasshi 2006; 126:521 – 7.

44. Li H, Li H, Wang Y, et al. An intervention study to prevent gastric cancer by micro-selenium and large dose of allitridum. Chinese Med J 2004;117:1155 – 60.

45. Oltvai ZN, Milliman CL, Korsmeyer SJ. Bcl-2 heterodimerizes *in vivo* with a conserved homolog, Bax, that accelerates programmed cell death. Cell 1993;74:609 – 19.

46. Kiefer MC, Brauer MJ, Powers VC, et al. Modulation of apoptosis by the widely distributed Bcl-2 homologue Bak. Nature 1995;374:736 – 9.

47. Mazars A, Genesto O, Hickman J. The Bcl-2 family of proteins as drug targets. J Soc Biol 2005;199:253 – 65.

48. Yamaguchi H, Chen J, Bhalla K, Wang HG. Regulation of Bax activation and apoptotic response to microtubule-damaging agents by p53 transcription-dependent and -independent pathways. J Biol Chem 2004; 279:39431 – 7.

Molecular Cancer Therapeutics

Mitochondria-mediated apoptosis by diallyl trisulfide in human prostate cancer cells is associated with generation of reactive oxygen species and regulated by Bax/Bak

Young-Ae Kim, Dong Xiao, Hui Xiao, et al.

Mol Cancer Ther 2007;6:1599-1609.